Journal of Applied Physics

Effects of flexoelectricity and strain gradient on bending vibration characteristics of piezoelectric semiconductor nanowires

Cite as: J. Appl. Phys. **129**, 164301 (2021); https://doi.org/10.1063/5.0038782
Submitted: 26 November 2020 . Accepted: 07 April 2021 . Published Online: 22 April 2021

Minghao Zhao, Jianan Niu, Chunsheng Lu, Bingbing Wang, and Cuiying Fan

Journal of Applied Physics ARTICLE scitation.org/journal/jap

Effects of flexoelectricity and strain gradient on bending vibration characteristics of piezoelectric semiconductor nanowires

Cite as: J. Appl. Phys. **129**, 164301 (2021); doi: 10.1063/5.0038782
Submitted: 26 November 2020 · Accepted: 7 April 2021 ·
Published Online: 22 April 2021

Minghao Zhao,[1] Jianan Niu,[1] Chunsheng Lu,[2] Bingbing Wang,[1,a)] and Cuiying Fan[1,a)]

AFFILIATIONS

[1]School of Mechanics and Safety Engineering, Zhengzhou University, Zhengzhou 450001, China
[2]School of Civil and Mechanical Engineering, Curtin University, Perth, Western Australia 6845, Australia

[a)]**Authors to whom correspondence should be addressed:** bbwang@zzu.edu.cn and fancy@zzu.edu.cn

ABSTRACT

In this paper, the governing equation of a piezoelectric semiconductor (PSC) is derived after a consideration of flexoelectricity and the strain gradient effect. A one-dimensional first-order beam model is obtained through integration across its section. Based on this model, theoretical analysis is carried out for a cantilever PSC nanowire subjected to a time-harmonic transverse shear force. The effects of flexoelectricity and the strain gradient on bending vibration characteristics are investigated, including the natural frequencies and distributions of physical quantities. The results show that the strain gradient effect on the natural frequency and stiffness of a PSC nanowire is greater than that of flexoelectricity, while with regard to the influence on electric potential and carrier concentration, the reverse is true. Our findings shed light on the design and optimization of PSC devices such as energy harvesters at the nanoscale.

I. INTRODUCTION

The discovery of the piezoelectric effect in ZnO, CdS, and other semiconductor materials[1–3] has attracted research interest in piezoelectric semiconductors (PSCs). Generally, PSCs[4] refer to a class of materials with both piezoelectricity and semiconductor properties. Therefore, when a load-induced deformation is applied on a PSC structure, the electric field caused by piezoelectricity drives charge carriers into motion or redistribution,[5] which control the gate in electronic devices such as transistors[6] or logical circuits.[7] Thus, PSCs can be used to develop smart microelectronic devices with modern functions,[8] for example, piezoelectric field-effect transistors,[9,10] nanogenerators,[11] photodetectors,[12] and light-emitting diodes.[13]

When PSCs are reduced to the nanoscale, it is necessary to take the size effect into account.[14] Several models such as the stress gradient,[15,16] strain gradient,[17–19] couple stress,[20–22] and integral-type theories[23,24] have been developed to describe the size effect. Among these, the strain gradient model, in which stresses depend on both strains and their gradients, proposed by Aifantis,[17] is the most convenient and widely used one for predicting the mechanical behavior of microbeams[25] and microplates.[26] Recently, the discovery of the flexoelectric effect in dielectric materials,[27] especially in ferroelectric thin films[28,29] and graphene nitride nanosheets,[30] has triggered more interest in studying the relationship between electric polarization and strain gradients. Generally speaking, the flexoelectric effect means strain gradients will induce electric polarization in media. Based on the continuum theory, polarization gradient-strain coupling in the free energy of elastic dielectrics was first introduced by Mindlin.[31] Then, Shen and Hu[32] established the variational principle for piezoelectric materials after considering strain gradients and flexoelectricity. Following this, mixed finite element methods,[33] mesh-free methods,[34] and B-spline methods[35] were developed to investigate the flexoelectricity in piezoelectric materials. However, there are relatively few studies on the strain gradient and flexoelectricity of PSCs. For instance, Liu *et al.*[36] analyzed the potential distribution of ZnO nanowires and found that, if semi-conductive properties are not considered, the flexoelectric effect has a large influence on potential. The potential distribution of PSC structures was investigated under the flexoelectric effect of low order stresses but without strain gradients.[37] The theoretical solution of a PSC nanowire under tension was derived,[38,39] in which both the strain gradient and flexoelectric effect are considered.[40]

In practical engineering, most devices function under dynamic environments. Therefore, it is pivotal to understand their dynamic characteristics such as the free frequency and vibration modes.[41] Yang *et al.*[42] analyzed Lamb waves by considering bending electrical properties and strain gradient elasticity in piezoelectric materials. Dynamic analyses of PSC beams and plates were carried out.[43–45] Here, it is worth noting that, in these studies, the strain gradient and the flexoelectric effect were ignored. As mentioned above, however, both the strain gradient and flexoelectric effect in micro- or nanoscales are significant and they significantly affect the dynamic characteristics of PSCs.

In this paper, a one-dimensional PSC model after taking both strain gradient and the flexoelectric effect into account is established by using the first-order beam theory. The paper is organized as follows. The basic equations and boundary conditions of a solid PSC are first described in Sec. II, with its degeneration to a one-dimensional beam model given in Sec. III. Then, theoretical solutions of a cantilever PSC nanowire are obtained under a time-harmonic transverse shear force in Sec. IV. Next, the influence of the strain gradient and flexoelectric effects on the dynamic characteristics of PSC nanowires is discussed in Sec. V. Finally, main conclusions are drawn in Sec. VI.

II. BASIC EQUATIONS AND BOUNDARY CONDITIONS

Based on the linear piezoelectric theory, the internal energy density with flexoelectricity and strain gradient[33] is expressed as

$$h = \frac{1}{2}\sigma_{ij}\varepsilon_{ij} + \frac{1}{2}\tau_{ijk}\eta_{ijk} - \frac{1}{2}D_iE_i - \frac{1}{2}G_{ji}E_{i,j}, \tag{1}$$

where ε_{ij}, η_{ijk}, and E_i are the strain, strain gradient, and electric fields, respectively. σ_{ij} is the classical stress tensor and D_i is the electric displacement vector. G_{ij} is the higher-order displacement vector, and τ_{ijm} is the higher-order stress tensor. Here, the strain tensor, the strain gradient tensor, and the electric field vector are defined as

$$\varepsilon_{ij} = \frac{1}{2}(u_{i,j} + u_{j,i}), \tag{2a}$$

$$\eta_{ijk} = \varepsilon_{ij,k}, \tag{2b}$$

$$E_i = -\phi_{,i}, \tag{2c}$$

where u and ϕ are the mechanical displacement and electric potential, respectively. The total enthalpy[33] is

$$R = \int_\Omega h dv - C, \tag{3}$$

where $C = \int_\Omega b_k u_k dv + \int_{\partial\Omega t} \bar{t}_k u_k ds + \int_{\partial\Omega r} \bar{r}_k \gamma_k ds - \int_{\partial\Omega q} \bar{q}\varphi ds - \int_{\partial\Omega w} \bar{\omega}\theta ds$ is work done by external forces. b_k, γ_k, and θ are the body force, normal derivatives of displacement, and electric potential, respectively. $\bar{t}_k$, $\bar{r}_k$, $\bar{q}$, and $\bar{\omega}$ are the prescribed traction force, higher-order traction force, electric displacement, and higher-order electric displacement on the corresponding boundaries, respectively.

Given that the frequency of an external load is much lower than the characteristic frequency of an electromagnetic field, the quasi-static approximation of the first Maxwell equation can be introduced. Therefore, the kinetic energy is

$$K = \frac{1}{2}\int_\Omega \rho \dot{u}_i \dot{u}_i dv, \tag{4}$$

where ρ is the density. According to the Hamilton principle, $\int_0^t (\delta R + \delta K) d\tau = 0$, governing equations can be represented by

$$(\sigma_{ij} - \tau_{ijm,m})_{,j} = \rho \ddot{u}_i, \tag{5a}$$

$$D_{i,i} - G_{ji,ij} = 0, \tag{5b}$$

with the following boundary conditions[33]:

(1) The traction and higher-order traction boundary conditions can be given as

$$\bar{t}_k = (\sigma_{ij} - \tau_{ijm,m})\bar{n}_j + (\Delta_l n_l)\tau_{ijm}\bar{n}_m\bar{n}_j - \Delta_j(\tau_{ijm}\bar{n}_m),$$

$$\bar{r}_k = \tau_{ijm}\bar{n}_m\bar{n}_j.$$

(2) The displacement and displacement normal derivatives boundary conditions can be given as

$$\bar{u}_k = u_k,$$

$$\bar{\gamma}_k = u_{k,i}\bar{n}_i.$$

(3) The electric displacement and higher-order electric displacement boundary conditions can be given as

$$\bar{q} = D_i\bar{n}_i - G_{ij,j}\bar{n}_i - \nabla_j^t(G_{ij}\bar{n}_i) + (\nabla_i^t\bar{n}_l)G_{ij}\bar{n}_i\bar{n}_j,$$

$$\bar{\omega} = -G_{ij}\bar{n}_i\bar{n}_j.$$

(4) The electric potential and electric potential normal derivatives boundary conditions can be given as

$$\bar{\phi} = \phi,$$

$$\bar{\theta} = -\phi_{,k}\bar{n}_k.$$

Here, $\bar{n}_i$ is the outward unit normal vector of boundary surfaces. For a general linear piezoelectric material, the enthalpy density[33] is expressed as

$$h = \frac{1}{2}c_{ijkl}\varepsilon_{ij}\varepsilon_{kl} + \frac{1}{2}l_{ijklmn}\eta_{ijk}\eta_{lmn} - e_{ijk}E_i\varepsilon_{jk} - f_{ijkl}E_i\eta_{jkl} + d_{ijkl}E_{j,i}\varepsilon_{kl} - \kappa_{ij}\frac{1}{2}E_iE_j, \tag{6}$$

in which these terms, respectively, refer to the energy densities of strain, strain gradient, piezoelectricity, direct flexoelectricity,

converse flexoelectricity, and the Maxwell self-field. c_{ijkl} and l_{ijkmnl} are the material parameter tensors. e_{ijk} is the piezoelectric coefficient tensor. f_{ijkl} and d_{ijkl} are direct and converse flexoelectric coefficients. κ_{ij} is the dielectric constant.

In terms of the variation of internal energy density, we have the constitutive equations

$$\sigma_{ij} = c_{ijks}\varepsilon_{ks} - e_{ijk}E_k, \tag{7a}$$

$$\tau_{ijm} = -f_{kijm}E_k + l_{ijmkns}\eta_{kns}, \tag{7b}$$

$$D_i = \kappa_{ij}E_j + e_{jki}\varepsilon_{jk} + f_{ijks}\eta_{jks}, \tag{7c}$$

$$G_{ij} = d_{ijkl}\varepsilon_{kl}. \tag{7d}$$

Here, based on Mindlin's strain gradient elasticity theory, the simplest variant of the higher-order elastic tensor is

$$l_{ijmkns} = g^2 c_{ijkn}\delta_{sm}, \tag{8}$$

where g is an internal scale parameter.

For PSCs, the semiconductor property should be considered besides piezoelectricity. Therefore, the charge conservation equation[46] is represented as

$$J^n_{i,i} = q\dot{n}, \tag{9}$$

where J^n_i is the hole current densities, n is the concentration of electrons, and $q = 1.6\times10^{-19}$ C is the electronic charge. The corresponding natural boundary condition is

$$J^n_i \bar{n}_i = \bar{J}, \tag{10}$$

where $\bar{J}$ is the given electric current.

In the case of a small change of electrons, the linear constitutive equation[44] for current densities is

$$J^n_i = qn_0\mu^n_{ij}E_j + qd^n_{ij}n_{,j}, \tag{11}$$

where n_0, μ^n_{ij}, and d^n_{ij} are the initial electron concentration, carrier mobility, and carrier diffusion constants of the n-type semiconductor, respectively. In addition, Eq. (5b) should be modified without the high-order electric displacement, as

$$D_{i,i} = -q\Delta n, \tag{12}$$

where $\Delta n = n - n_0$ is the perturbation of electron concentration.

III. ONE-DIMENSIONAL EQUATIONS

Let us consider a PSC nanowire. As illustrated in Fig. 1, the left end of the PSC nanowire is fixed, and a time-harmonic transverse shear force is applied at its right end. Since the slenderness ratio $L/a \gg 1$, a one-dimensional beam model can be assumed. According to the first-order beam theory, the relevant mechanical displacements, electric potential, and carrier concentrations are

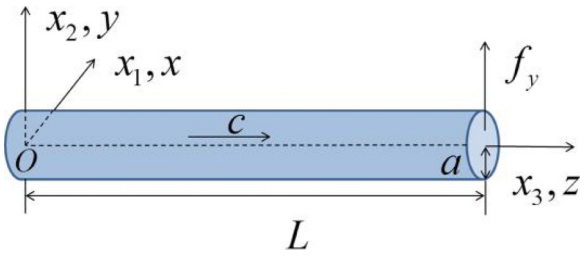

FIG. 1. Schematic illustration of a PSC nanowire, where a is the radius, L is the length, and c axis is along the x_3 direction.

approximated as

$$u_2(x, t) \cong w(x_3, t), \tag{13a}$$

$$u_3(x, t) \cong x_2\psi(x_3, t), \tag{13b}$$

$$\phi(x, t) \cong x_2\phi^{(1)}(x_3, t), \tag{13c}$$

$$\Delta n(x, t) \cong x_2 n^{(1)}(x_3, t), \tag{13d}$$

where $w(x_3,t)$ and $\psi(x_3,t)$ stand for the lateral deflection and rotation angle of the nanowire, and $\phi(1)(x_3,t)$ and $n(1)(x_3,t)$ are the lateral electric potential and electron concentration, respectively. For a cubic crystal, there are three independent flexoelectric coefficients,[47] i.e.,

$$f_{3333} = f_{11}, \quad f_{2323} = f_{3232} = f_{2332} = f_{44}, \quad f_{2233} = f_{3322} = f_{12}. \tag{14}$$

Then, from Eqs. (7) and (11), we can obtain

$$\sigma_{33} = c_{33}\varepsilon_{33} - e_{33}E_3, \tag{15a}$$

$$\sigma_{23} = c_{44}\varepsilon_{23} - e_{15}E_2, \tag{15b}$$

$$D_2 = e_{15}\varepsilon_{23} + k_{11}E_2 + f_{44}\varepsilon_{33,2} + f_{12}\varepsilon_{23,3}, \tag{15c}$$

$$D_3 = e_{33}\varepsilon_{33} + k_{33}E_3 + f_{11}\varepsilon_{33,3}, \tag{15d}$$

$$J^n_2 = qn_0\mu^n_{11}E_2 + qd^n_{11}n_{,2}, \tag{15e}$$

$$J^n_3 = qn_0\mu^n_{33}E_3 + qd^n_{33}x_2 n_{,3}, \tag{15f}$$

and the higher-order stresses are expressed as

$$\tau_{232} = -f_{44}E_3 + g^2 c_{44}\varepsilon_{23,2}, \tag{16a}$$

$$\tau_{233} = -f_{12}E_2 + g^2 c_{44}\varepsilon_{23,3}, \tag{16b}$$

$$\tau_{332} = -f_{44}E_2 + g^2 c_{33}\varepsilon_{33,2}, \tag{16c}$$

$$\tau_{333} = -f_{11}E_3 + g^2 c_{33}\varepsilon_{33,3}. \tag{16d}$$

Then, by integrating Eq. (5), Eq. (9), and their moment forms along the cross section, we have the equilibrium equation,

$$Q_{,3} = \rho A\ddot{w}, \tag{17a}$$

$$M_{,3} - Q = \rho I\ddot{\psi}, \tag{17b}$$

$$D^{(1)}_{3,3} - D^{(0)}_2 = -qIn^{(1)}, \tag{17c}$$

$$J^{n(1)}_{3,3} - J^{n(0)}_2 = qI\dot{n}^{(1)}, \tag{17d}$$

where I and A are the moment of inertia and area of the cross section that can be calculated by

$$I = \int_A x_2^2 dA = \frac{\pi a^4}{4}, \tag{18a}$$

$$A = \pi a^2. \tag{18b}$$

From Eqs. (14) and (15), the one-dimensional constitutive equation is

$$\begin{aligned} Q &= \int (\sigma_{23} - \tau_{232,2} - \tau_{233,3})dA \\ &= c_{44}A(w_{,3} - g^2 w_{,333}) + c_{44}A(\psi - g^2\psi_{,33}) \\ &\quad + e_{15}A\phi^{(1)} - (f_{12} + f_{44})A\phi^{(1)}_{,3}, \end{aligned} \tag{19a}$$

$$\begin{aligned} M &= \int x_2(\sigma_{33} - \tau_{332,2} - \tau_{333,3})dA \\ &= c_{33}I(\psi_{,3} - g^2\psi_{,333}) + e_{33}I\phi^{(1)}_{,3} - f_{11}I\phi^{(1)}_{,33}, \end{aligned} \tag{19b}$$

$$Q^h = \int_A \tau_{233}dA = f_{12}A\phi^{(1)} + c_{44}Ag^2(w_{,33} + \psi_{,3}), \tag{19c}$$

$$M^h = \int_A x_2\tau_{333}dA = f_{11}I\phi^{(1)}_{,3} + g^2 c_{33}I\psi_{,33}, \tag{19d}$$

$$\begin{aligned} D^{(0)}_2 &= \int D_2 dA \\ &= (e_{15}Aw_{,3} + f_{12}Aw_{,33}) + [e_{15}A\psi + (f_{12} + f_{44})A\psi_{,3}] - \kappa_{11}A\phi^{(1)}, \end{aligned} \tag{19e}$$

$$D^{(1)}_3 = \int x_2 D_3 dA = e_{33}I\psi_{,3} + f_{11}I\psi_{,33} - \kappa_{33}I\phi^{(1)}_{,3}, \tag{19f}$$

$$J^{n(0)}_2 = \int J^n_2 dA = -qn_0\mu^n_{11}A\phi^{(1)} + qd^n_{11}An^{(1)}, \tag{19g}$$

$$J^{n(1)}_3 = \int x_2 J^n_3 dA = -qn_0\mu^n_{33}I\phi^{(1)}_{,3} + qd^n_{33}In^{(1)}_{,3}, \tag{19h}$$

where Q, M, Q^h, M^h, $D^{(0)}_2$, $D^{(1)}_3$, $J^{n(0)}_2$, and $J^{n(1)}_3$ are the shear force, bending moment, high-order shear force, high-order bending moment, and zero- and first-order electric displacement and carrier concentration, respectively. The corresponding boundary conditions for one-dimensional PSC beams can be determined by integrating the boundary conditions in a three-dimensional case along the cross section.

IV. TIME-HARMONIC BENDING FORCED VIBRATION

In terms of generalized displacement, substituting Eq. (19) into Eq. (17) leads to the governing equation,

$$\begin{aligned} &c_{44}A(w_{,33} - g^2 w_{,3333}) + c_{44}A(\psi_{,3} - g^2\psi_{,333}) + e_{15}A\phi^{(1)}_{,3} \\ &\quad - (f_{12} + f_{44})A\phi^{(1)}_{,33} = \rho A\ddot{w}, \end{aligned} \tag{20a}$$

$$\begin{aligned} &c_{33}I(\psi_{,33} - g^2\psi_{,3333}) + e_{33}I\phi^{(1)}_{,33} - f_{11}I\phi^{(1)}_{,333} - c_{44}A(w_{,3} - g^2 w_{,333}) \\ &\quad - c_{44}A(\psi - g^2\psi_{,33}) - e_{15}A\phi^{(1)} + (f_{12} + f_{44})A\phi^{(1)}_{,3} = \rho I\ddot{\psi}, \end{aligned} \tag{20b}$$

$$\begin{aligned} &e_{33}I\psi_{,33} + f_{11}I\psi_{,333} - \kappa_{33}I\phi^{(1)}_{,33} - e_{15}Aw_{,3} + f_{12}Aw_{,33} - e_{15}A\psi \\ &\quad - (f_{12} + f_{44})A\psi_{,3} + \kappa_{11}A\phi^{(1)} = -qIn^{(1)}, \end{aligned} \tag{20c}$$

$$(-qn_0\mu^n_{33}I\phi^{(1)}_{,33} + qd^n_{33}In^{(1)}_{,33}) - (-qn_0\mu^n_{11}A\phi^{(1)} + qd^n_{11}An^{(1)}) = qI\dot{n}^{(1)}. \tag{20d}$$

Therefore, as illustrated in Fig. 1, the boundary conditions are

$$w(0) = 0, \qquad Q(L) = f_y, \tag{21a}$$

$$\psi(0) = 0, \qquad M(L) = 0, \tag{21b}$$

$$w_{,3}(0) = 0, \qquad Q^h(L) = 0, \tag{21c}$$

$$\psi_{,3}(0) = 0, \qquad M^h(L) = 0, \tag{21d}$$

$$D^{(1)}_3(0) = 0, \qquad D^{(1)}_3(L) = 0, \tag{21e}$$

$$J^{(1)}_3(0) = 0, \qquad J^{(1)}_3(L) = 0. \tag{21f}$$

For a time-harmonic bending vibration, a force is given by

$$f_y = F\exp(i\omega t), \tag{22}$$

where F and ω are the magnitude and frequency of the force, respectively, and i is the imaginary unit. Then, the harmonic

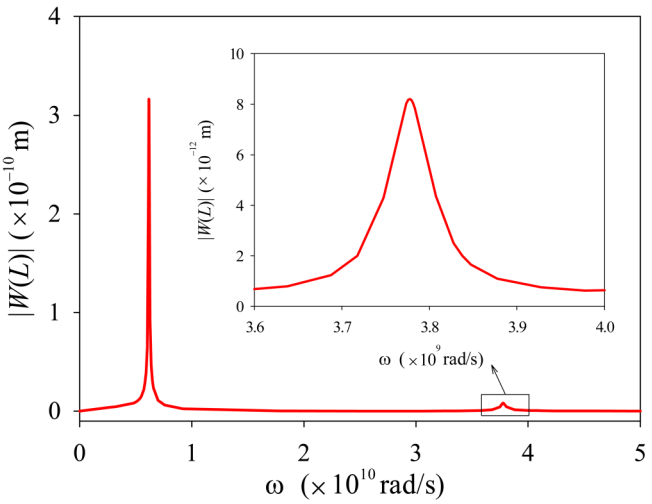

FIG. 2. The relationship between the drive frequency and the nanowire end displacement with two resonances $\omega_1 = 6.1764 \times 10^8$ rad/s and $\omega_2 = 3.7776 \times 10^9$ rad/s.

solution can be written as

$$\{w, \psi, \phi^{(1)}, n^{(1)}\} = \{W, \Psi, \Phi, N\}\exp(i\omega t). \tag{23}$$

Substituting Eq. (23) into Eq. (20) leads to

$$c_{44}A(W_{,33} - g^2 W_{,3333}) + c_{44}A(\Psi_{,3} - g^2\Psi_{,333}) + e_{15}A\Phi_{,3} - (f_{12} + f_{44})A\Phi_{,33} + \rho A\omega^2 W = 0, \tag{24a}$$

$$c_{33}I(\Psi_{,33} - g^2\Psi_{,3333}) + e_{33}I\Phi_{,33} - f_{11}I\Phi_{,333} - c_{44}A(W_{,3} - g^2 W_{,333}) - c_{44}A(\Psi - g^2\Psi_{,33}) - e_{15}A\Phi + (f_{12} + f_{44})A\Phi_{,3} + \rho\omega^2 I\Psi = 0, \tag{24b}$$

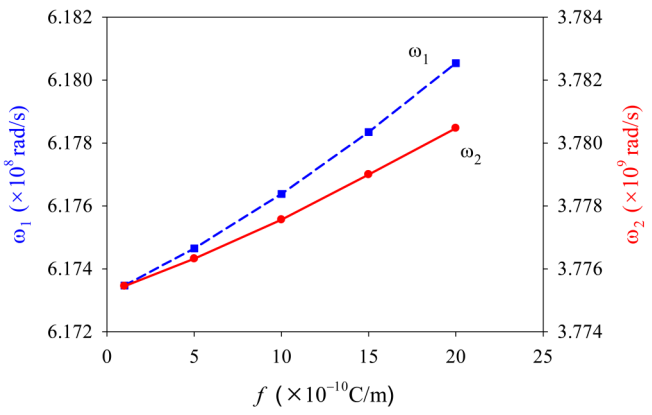

FIG. 3. Fundamental and second-order natural frequencies vs flexoelectric coefficient f in the case of $g = 10^{-9}$ m and $n_0 = 10^{23}$ m^{-3}.

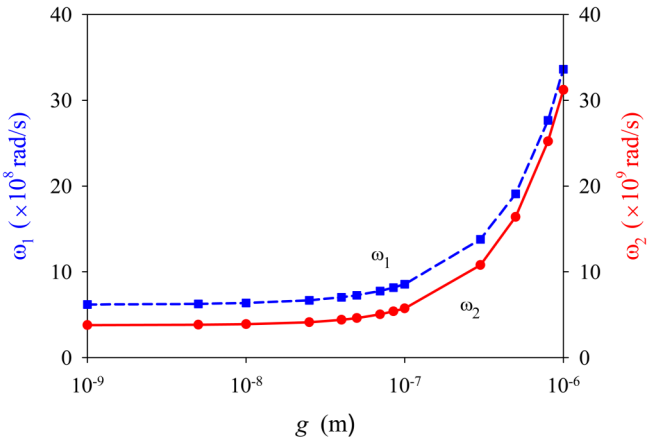

FIG. 4. Fundamental and second-order natural frequencies vs internal scale parameter g in the case of $f = 10^{-9}$ C/m and $n_0 = 10^{23}$ m^{-3}.

$$e_{33}I\Psi_{,33} + f_{11}I\Psi_{,333} - \kappa_{33}I\Phi_{,33} - (e_{15}AW_{,3} + f_{12}AW_{,33}) - e_{15}A\Psi - (f_{12} + f_{44})A\Psi_{,3} + \kappa_{11}A\Phi + qIN = 0, \tag{24c}$$

$$(-qn_0\mu_{33}^n I\Phi_{,33} + qd_{33}^n IN_{,33}) - (-qn_0\mu_{11}^n A\Phi + qd_{11}^n AN) - i\omega qIN = 0. \tag{24d}$$

The solution of Eq. (24) is

$$\{W, \Psi, \Phi, N\} = \{C_1, C_2, C_3, C_4\}\exp(\lambda x_3). \tag{25}$$

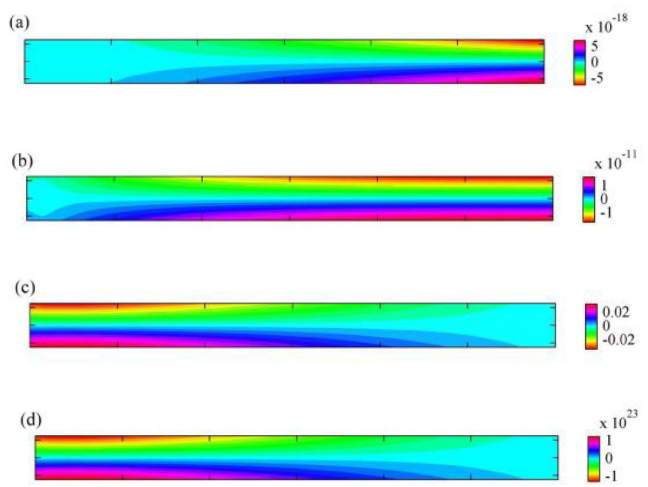

FIG. 5. Contours of the imaginary parts of (a) deflection $W(x_3)$; (b) shear deformation $\Psi(x_3)$; (c) electric potential $\Phi(x_3)$; and (d) carrier concentration $N(x_3)$ along the longitudinal section in the case of $\omega = \omega_1$, $g = 10^{-9}$ m and $f = 10^{-7}$ C/m.

Substituting Eq. (25) into Eq. (24) leads to the following equation group:

$$c_{44}A(\lambda^2C_1 - g^2\lambda^4C_1) + c_{44}A(\lambda C_2 - g^2\lambda^3C_2) + e_{15}A\lambda C_3 - (f_{12}+f_{44})A\lambda^2C_3 + \rho A\omega^2C_1 = 0, \tag{26a}$$

$$c_{33}I(\lambda^2C_2 - g^2\lambda^4C_2) + e_{33}I\lambda^2C_3 - f_{11}I\lambda^3C_3 - c_{44}A(\lambda C_1 - g^2\lambda^3C_1) - c_{44}A(C_2 - g^2\lambda^2C_2) - e_{15}AC_3 + (f_{12}+f_{44})A\lambda C_3 + \rho\omega^2IC_2 = 0, \tag{26b}$$

$$(e_{33}I\lambda^2C_2 + f_{11}I\lambda^3C_2 - \kappa_{33}I\lambda^2C_3) - (e_{15}A\lambda C_1 + f_{12}A\lambda^2C_1) - e_{15}AC_2 - (f_{12}+f_{44})A\lambda C_2 + \kappa_{11}AC_3 + qIC_4 = 0, \tag{26c}$$

$$-qn_0\mu_{33}^nI\lambda^2C_3 + qd_{33}^nI\lambda^2C_4 + qn_0\mu_{11}^nAC_3 - qd_{11}^nAC_4 - i\omega qIC_4 = 0. \tag{26d}$$

Obviously, there are four linear homogeneous algebraic equations about C_1–C_4. In order to have nontrivial solutions, the determinant of the coefficient matrix of Eq. (26) must be zero. Since the

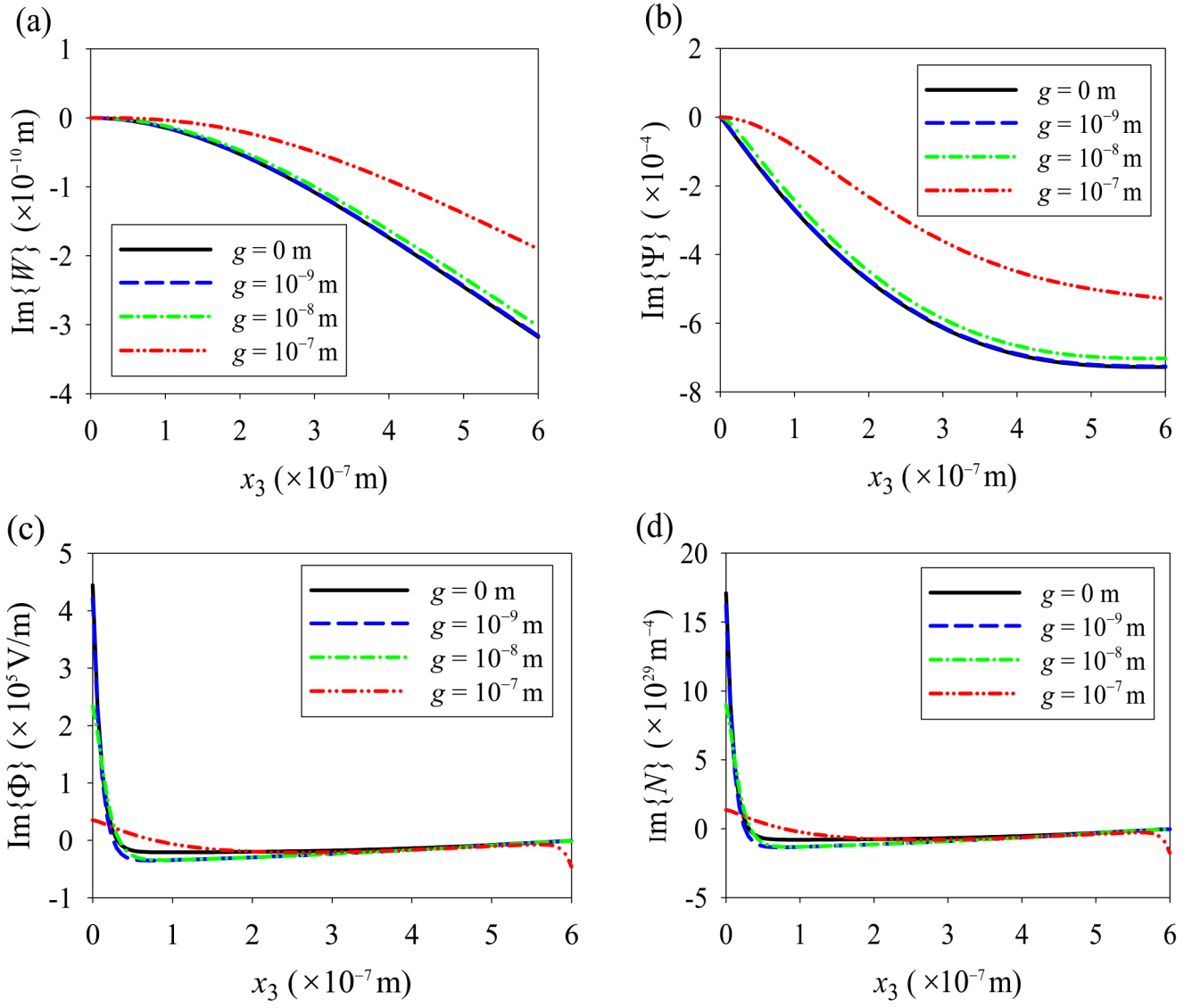

FIG. 6. Distribution of the imaginary parts of (a) deflection $W(x_3)$; (b) shear deformation $\Psi(x_3)$; (c) electric potential $\Phi(x_3)$; and (d) carrier concentration $N(x_3)$ with different internal scale parameters in the case of $\omega = \omega_1$ and $f = 10^{-9}$ C/m.

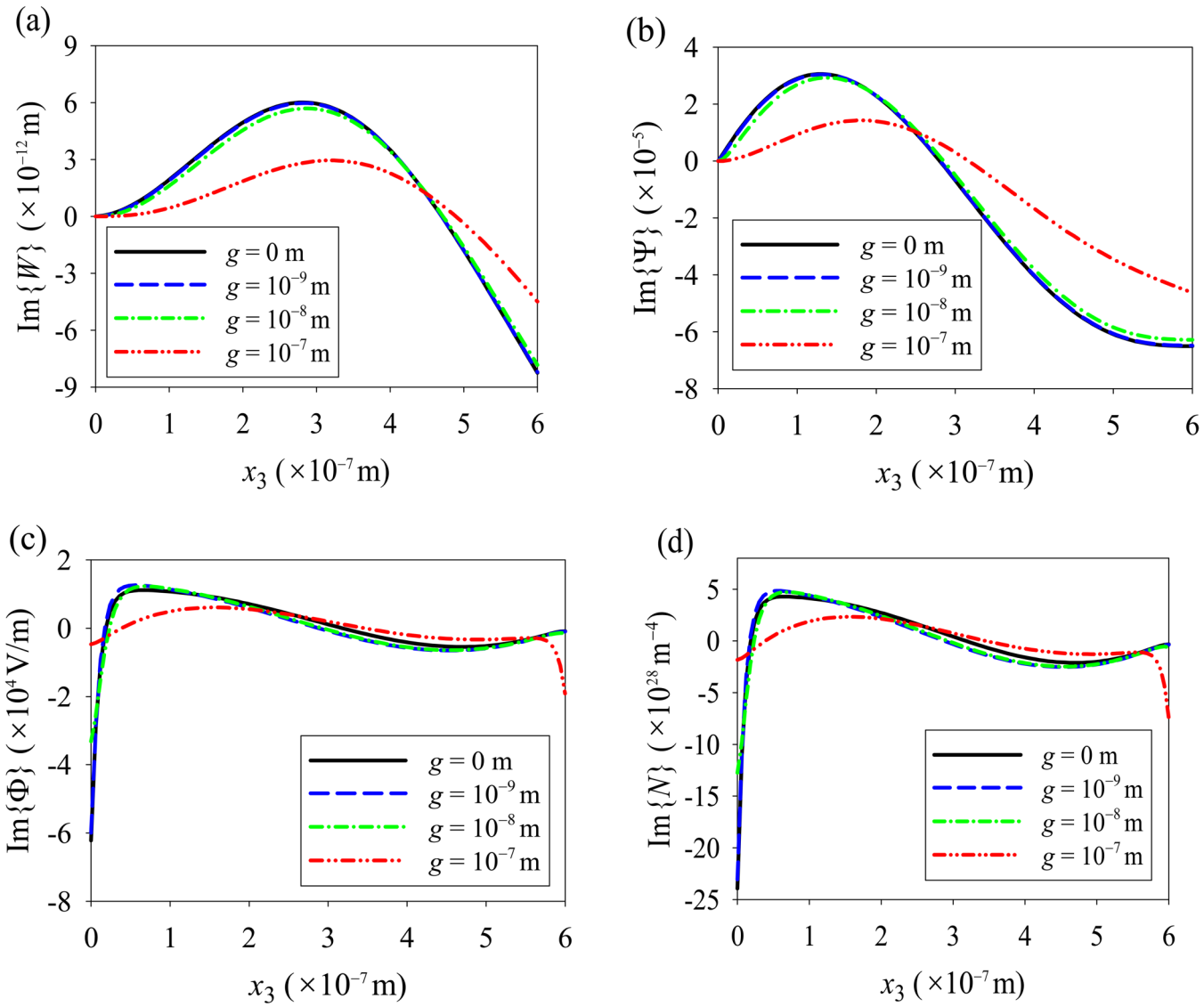

FIG. 7. Distribution of the imaginary parts of (a) deflection $W(x_3)$; (b) shear deformation $\Psi(x_3)$; (c) electric potential $\Phi(x_3)$; and (d) carrier concentration $N(x_3)$ with different internal scale parameters in the case of $\omega = \omega_2$ and $f = 10^{-9}$ C/m.

determinant is a polynomial of 12 order, 12 roots, noted by λ^m, can be determined. Then, substituting λ^m into Eq. (26) separately, we can obtain the ratios among $C_1^m - C_4^m$. Finally, the general solution can be written as

$$\begin{Bmatrix} W \\ \Psi \\ \Phi \\ N \end{Bmatrix} = \sum_{m=1}^{12} H^{(m)} \begin{Bmatrix} C_1^{(m)} \\ C_2^{(m)} \\ C_3^{(m)} \\ C_4^{(m)} \end{Bmatrix} \exp(\lambda^{(m)} x_3), \tag{27}$$

where H^m are the 12 constants that can be determined by 12 boundary conditions [Eq. (21)].

V. RESULTS AND DISCUSSION

As an example, let us consider a ZnO nanowire with the length $L = 600$ nm and the radius $a = 25$ nm. The effective material constants are from Ref. 44. The initial electron concentration was chosen as $n_0 = N_D^+ = 10^{23}$ m^{-3}, and the applied force is $F = 0.002$ nN. To investigate the flexoelectricity and strain gradient effect, flexoelectric coefficients were tested in the range of 0.1×10^{-9} to

2×10^{-9} C/m and internal scale parameters were chosen from 10^{-9} to 10^{-6} m. The flexoelectric coefficients in the semiconductor ZnO are still unknown, so we refer to the flexoelectric coefficients in the value range of other materials[48,49] to test the flexoelectric effect. The values of three flexoelectricity coefficients were taken to be $f = f_{11} = f_{12} = f_{44}$ for simplicity.[50]

As shown in Fig. 2, by the resonance method, fundamental and second frequencies in the case of $f = 10^{-9}$ C/m and $g = 10^{-9}$ m can be obtained, i.e., $\omega_1 = 6.1764 \times 10^8$ rad/s and $\omega_2 = 3.7776 \times 10^9$ rad/s. These are almost consistent with the classical results[44] of $\omega_{1c} = 6.1570 \times 10^8$ rad/s and $\omega_{2c} = 3.7651 \times 10^9$ rad/s.

It is observed in Fig. 3 that in the case of $g = 10^{-9}$ m, as f increases, both fundamental and second frequencies increase. In addition, when the flexoelectric coefficient is in the range of 0.1×10^{-9} to 2×10^{-9} C/m, the maximum difference $|(\omega_1 - \omega_{1c})/\omega_{1c}|$ is 0.38%, and $|(\omega_2 - \omega_{2c})/\omega_{2c}|$ is 0.41%. From Fig. 4, it is seen that when the flexoelectric coefficient f is fixed as 10^{-9} C/m, both fundamental and second frequencies increase with the internal scale parameter g,

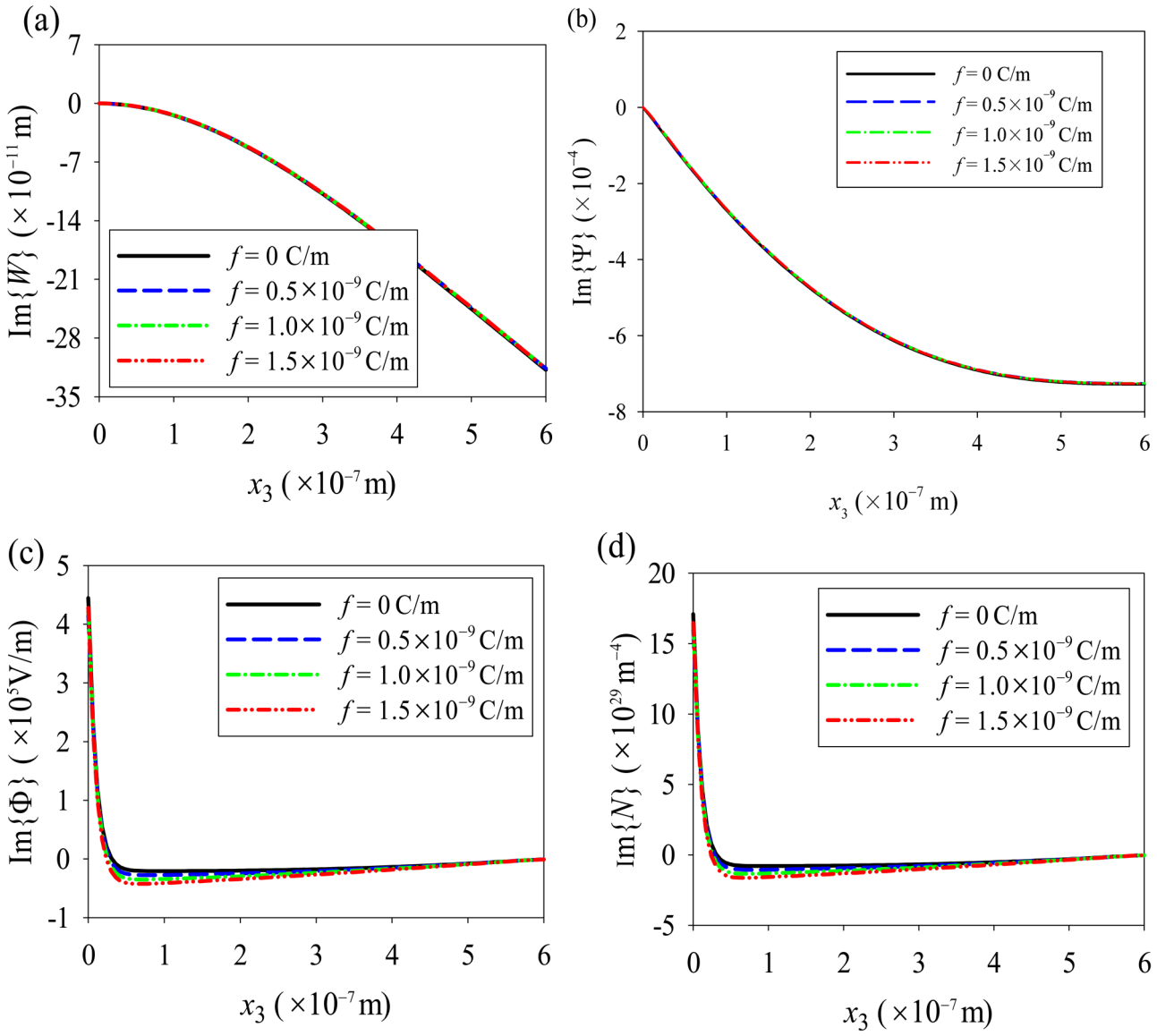

FIG. 8. Distribution of the imaginary parts of (a) deflection $W(x_3)$; (b) shear deformation $\Psi(x_3)$; (c) electric potential $\Phi(x_3)$; and (d) carrier concentration $N(x_3)$ with different flexoelectric coefficients in the case of $\omega = \omega_1$ and $g = 10^{-9}$ m.

implying that the strain gradient effect can improve the stiffness of a PSC nanowire. Here, the maximum differences of $|(\omega_1 - \omega_{1c})/\omega_{1c}|$ and $|(\omega_2 - \omega_{2c})/\omega_{2c}|$ can reach 446% and 729% in the range of 10^{-9} to 10^{-6} m. We have separately checked the growth rate of the vibration frequency as the flexoelectric coefficient and the internal scale parameter become larger, and the results show that the strain gradient effect on natural frequencies is higher than that of flexoelectricity. This shows that the strain gradient effect on the stiffness of a PSC nanowire is larger than that of flexoelectricity.

The imaginary parts of deflection are much larger than the real parts; therefore, only the imaginary parts are focused. In the case of $\omega = \omega_1$, $g = 10^{-9}$ m, and $f = 10^{-9}$ C/m, the contours of deflection, rotation, electric potential, and carrier concentration along the longitudinal section are shown in Fig. 5, which also agree with the classical results.[44] In the case of $\omega = \omega_1$, it is observed from Fig. 6 that, for a small value of the internal scale parameter $g = 10^{-9}$ m, the distributions of deflection, rotation, electric potential, and carrier concentration coincide with those without considering the strain gradient

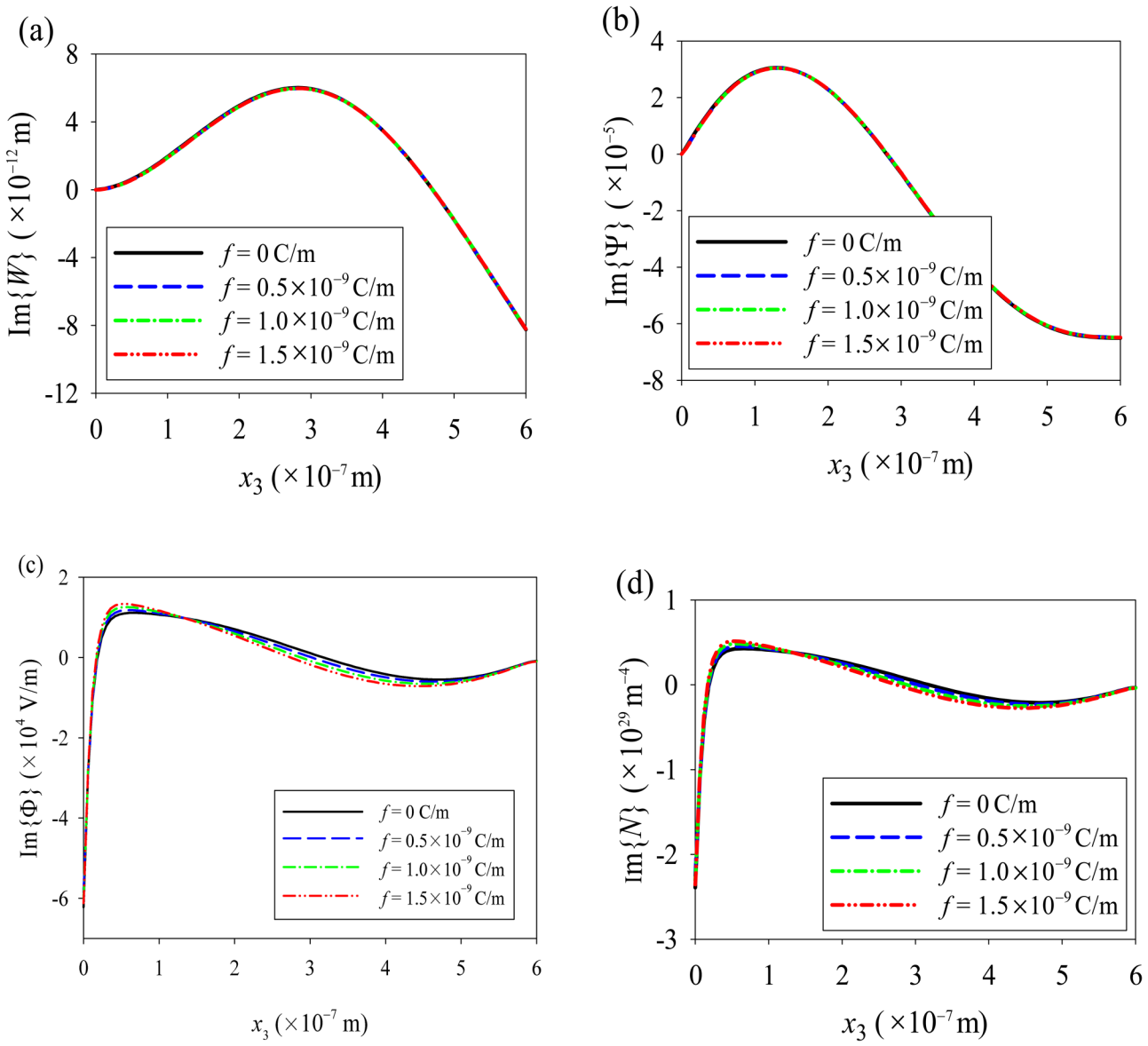

FIG. 9. Distribution of the imaginary parts of (a) deflection $W(x_3)$; (b) shear deformation $\Psi(x_3)$; (c) electric potential $\Phi(x_3)$; and (d) carrier concentration $N(x_3)$ with different flexoelectric coefficients in the case of $\omega = \omega_2$ and $g = 10^{-9}$ m.

effect. As the value of g increases, the deflection and rotation decrease, while the electric potential and carrier concentration decrease at the fixed end and increase at the other end. A similar phenomenon was observed in the case of $\omega = \omega_2$, as shown in Fig. 7.

Furthermore, the influence of flexoelectric coefficients on the distributions of physical quantities was investigated. As seen in Fig. 8, in the case of $g = 10^{-9}$ m, the distribution trends of deflection, rotation, electric potential, and carrier concentration coincide with those without considering flexoelectricity. It is observed that the deflection and rotation decrease as the value of f increases, implying that flexoelectricity can improve the stiffness of a PSC nanowire. The distributions of electric potential and carrier concentration move down as f increases. Taking the influence of a large carrier concentration at the fixed end on the linear constitutive equation[44] into account, only solutions far away from the fixed end are considered. Obviously, the electric potential and carrier concentration increase with f. A similar phenomenon is observed in the case of $\omega = \omega_2$ (see Fig. 9).

Finally, by comparing Figs. 8(a) and 8(b) with Figs. 8(c) and 8(d), it is seen that the effect of flexoelectricity on the electric potential and carrier concentration is more obvious. This is because flexoelectricity is caused by the coupling effect of force and electricity, which reflects more on electrical properties.

VI. CONCLUSIONS

In this paper, the governing equation of a PSC nanowire has been derived after considering both flexoelectricity and the strain gradient effect. Theoretical solutions of deflection, rotation, electric potential, and carrier concentration have been given for a cantilever PSC nanowire subjected to a time-harmonic shear force. The main conclusions can be summarized as follows:

(1) As the flexoelectric coefficient and the internal scale parameter increase, natural frequencies also increase.
(2) The stiffness of a PSC nanowire increases with the flexoelectric coefficient and internal scale parameter, and the influence of the strain gradient effect on the stiffness and fundamental and second-order natural frequencies is larger than that of flexoelectricity.
(3) The electric potential and carrier concentration at the part far away from the fixed end of a PSC nanowire increase with the flexoelectric coefficient and internal scale parameter.
(4) The influence of flexoelectricity on the electric potential and carrier concentration is greater than that of deflection and rotation.

ACKNOWLEDGMENTS

This work has been supported by the National Natural Science Foundation of China (NNSFC) (No. 11572289).

DATA AVAILABILITY

The data that support the findings of this study are available from the corresponding author upon reasonable request.

REFERENCES

[1]A. R. Hutson, Phys. Rev. Lett. **4**, 505 (1960).
[2]A. R. Hutson and D. L. White, J. Appl. Phys. **33**, 40 (1962).
[3]D. L. White, "Amplification of Ultrasonic Waves in Piezoelectric Semiconductors," in *PTGMTT National Symposium Digest* **63**, 199 (1962).
[4]C. F. Pan, J. Y. Zhai, and Z. L. Wang, Chem. Rev. **119**, 9303 (2019).
[5]H. Nazemi, A. Joseph, J. Park, and A. Emadi, Sensors **19**, 1285 (2019).
[6]C. F. Wang, C. H. Wang, Z. L. Huang, and S. Xu, Adv. Mater. **30**, 1801368 (2018).
[7]A. Khan, R. Chakrabarty, and D. De, Microsyst. Technol. **23**, 4169 (2017).
[8]M. Mecklenburg, W. A. Hubbard, E. R. White, R. Dhall, S. B. Cronin, S. Aloni, and B. C. Regan, Science **347**, 629 (2015).
[9]Y. Yang, J. J. Qi, W. Guo, Y. S. Gu, Y. H. Huang, and Y. Zhang, Phys. Chem. Chem. Phys. **12**, 12415 (2010).
[10]X. D. Wang, J. Zhou, J. H. Song, J. Liu, N. S. Xu, and Z. L. Wang, Nano Lett. **6**, 2768 (2006).
[11]Z. L. Wang, Adv. Funct. Mater. **18**, 3553 (2008).
[12]Y. Guo, S. Zhou, Y. Z. Bai, and J. J. Zhao, Appl. Phys. Lett. **110**, 163102 (2017).
[13]A. Ahmed, M. Shehata, I. Hassan, Y. I. Abdelhak, E. Cigdem, M. El-Kady, Y. Ismail, and H. Mostafa, Nano Energy **74**, 104874 (2020).
[14]Z. L. Wang, W. Z. Wu, and C. Falconi, MRS Bull. **43**, 922 (2018).
[15]A. C. Eringen, J. Appl. Phys. **54**, 4703 (1983).
[16]A. Apuzzo, R. Barretta, M. Canadija, L. Feo, R. Luciano, and F. M. de Sciarra, Compos. B Eng. **108**, 315 (2017).
[17]E. C. Aifantis, Int. J. Eng. Sci. **30**, 1279 (1992).
[18]A. Apuzzo, R. Barretta, S. A. Faghidian, R. Luciano, and F. M. de Sciarra, Int. J. Eng. Sci. **133**, 99 (2018).
[19]R. Barretta, S. A. Faghidian, and F. M. de Sciarra, Int. J. Eng. Sci. **136**, 38 (2019).
[20]D. R. Mindlin and H. F. Tiersten, Arch. Ration. Mech. Anal. **11**, 415 (1962).
[21]R. A. Toupin, Arch. Ration. Mech. Anal. **11**, 385 (1962).
[22]Y. S. Li, E. Pan, and X. Liang, Int. J. Eng. Sci. **97**, 40 (2015).
[23]M. Di Paola, G. Failla, A. Pirrotta, A. Sofi, and M. Zingales, Philos. Trans. R. Soc. A. **371**, 20120433 (2013).
[24]M. Di Paola, G. Failla, and M. Zingales, J. Elasticity **97**, 103 (2009).
[25]S. L. Kong, S. J. Zhou, Z. F. Nie, and K. Wang, Int. J. Eng. Sci. **47**, 487 (2009).
[26]B. Babu and B. P. Patel, Compos. B Eng. **168**, 302 (2019).
[27]P. Zubko, G. Catalan, and A. K. Tagantsev, Annu. Rev. Mater. Res. **43**, 387 (2013).
[28]P. F. Yu, H. L. Wang, J. Y. Chen, and S. P. Shen, J. Mech. Phys. Solids **104**, 57 (2017).
[29]W. Y. Liu, F. Deng, S. X. Xie, S. P. Shen, and J. Y. Li, J. Mech. Phys. Solids **142**, 104020 (2020).
[30]P. Yu, F. M. Wang, T. A. Shifa, X. Y. Zhan, X. D. Lou, F. Xia, and J. He, Nano Energy **58**, 244 (2019).
[31]R. D. Mindlin, Int. J. Solids Struct. **4**, 637 (1968).
[32]S. P. Shen and S. L. Hu, J. Mech. Phys. Solids **58**, 665 (2010).
[33]F. Deng, Q. Deng, and S. P. Shen, J. Appl. Mech. **85**, 031009 (2018).
[34]A. Abdollahi, C. Peco, D. Millán, M. Arroyo, and I. Arias, J. Appl. Phys. **116**, 093502 (2014).
[35]X. Y. Zhuang, B. H. Nguyen, S. S. Nanthakumar, T. Q. Tran, N. Alajlan, and T. Rabczuk, Energies **13**, 1326 (2020).
[36]C. C. Liu, S. L. Hu, and S. P. Shen, Smart Mater. Struct. **21**, 115024 (2012).
[37]K. F. Wang and B. L. Wang, Nanotechnology **29**, 255405 (2018).
[38]M. H. Zhao, X. Liu, C. Y. Fan, C. S. Lu, and B. B. Wang, J. Appl. Phys. **127**, 085707 (2020).
[39]C. L. Zhang, X. Y. Wang, W. Q. Chen, and J. S. Yang, Smart Mater. Struct. **26**, 025030 (2017).
[40]G. L. Wang, J. X. Liu, X. L. Liu, W. J. Feng, and J. S. Yang, J. Appl. Phys. **124**, 094502 (2018).
[41]H. Safarpour, Z. E. Hajilak, and M. Habibi, Int. J. Mech. Mater. Des. **15**, 569 (2019).
[42]W. J. Yang, Q. Deng, X. Liang, and S. P. Shen, Smart Mater. Struct. **27**, 085003 (2018).

[43]P. C. Jiao, A. H. Alavi, W. Borchani, and N. Lajnef, Compos. Struct. **195**, 219 (2018).
[44]X. Y. Dai, F. Zhu, Z. H. Qian, and J. S. Yang, Nano Energy **43**, 22 (2018).
[45]S. S. Zhou, S. J. Zhou, B. L. Wang, and A. Q. Li, Appl. Math. Model. **41**, 462 (2017).
[46]R. R. Cheng, C. L. Zhang, W. Q. Chen, and J. S. Yang, J. Appl. Phys. **124**, 064506 (2018).
[47]R. Z. Zhang, X. Liang, and S. P. Shen, Meccanica **51**, 1181 (2016).
[48]J. Narvaez, F. Vasquez-Sancho, and G. Catalan, Nature **538**, 219 (2016).
[49]L. L. Shu, S. M. Ke, L. F. Fei, W. B. Hang, Z. G. Wang, J. H. Gong *et al.*, Nat. Mater. **19**, 605 (2020).
[50]L. L. Shu, X. Y. Wei, T. Pang, X. Yao, and C. L. Wang, J. Appl. Phys. **110**, 104106 (2011).